

# TOWARDS CALIBRATION OF GNSS RECEIVER HARDWARE DELAYS FOR IMPROVING GEODETIC REFERENCE SYSTEMS THROUGH CLOCK TIES. A REQUIREMENTS ANALYSIS FOR DEVELOPING A GNSS PSEUDOLITE TRANSMISSION CHAIN.



Alexandru Mihai Lăpădat (1), Jan Kodet (2), Thomas Pany (1)

(1) Institute of Space Technology and Space Applications (ISTA), University of the Bundeswehr Munich (UniBw), Germany  
 (2) Forschungseinrichtung Satellitengeodäsie, Technical University of Munich, Geodetic Observatory Wettzell, Germany



A.M.Lapadat@tudelft.nl

## PROBLEM STATEMENT

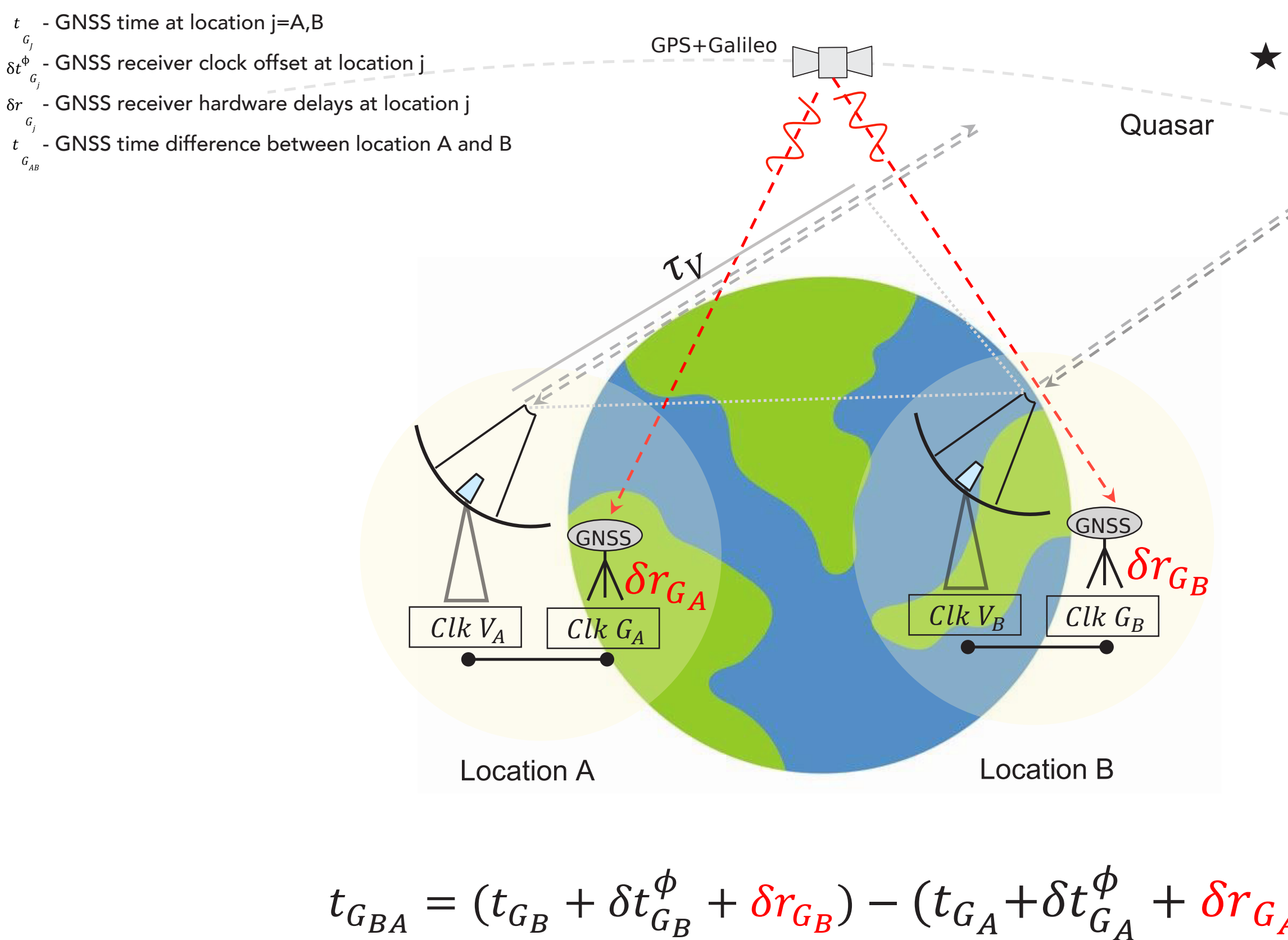


Figure 1: Global remote time transfer via inter-station clock differencing of VLBI ( $\tau_V$ , grey) and GNSS ( $t_{c_j}$ ) between observatory A and B. The two geodetic techniques at each observatory location are tied to the same time source,  $\tau_V \neq t_{G_{BA}}$  due to variable hardware delays ( $\delta r_{G_A}$  and  $\delta r_{G_B}$ ) that affect the GNSS clocks.

The increasing demand for Earth science applications presents challenges in enhancing geodetic reference frames. Current methods for defining these frames and the infrastructure at fundamental observatories are limited by systematic errors, such as variable hardware delays ( $\delta r_g$ ).

An application where the impact of variable hardware delays is clear is remote time transfer. Remote time transfer across the globe ( $t_{G_{BA}}$ ) is established on behalf of inter-station clock differencing of geodetic techniques such as the Very Long Baseline Interferometry (VLBI) or the Global Navigation Satellite Systems (GNSS). In theory, if VLBI and GNSS systems are geometrically tied and synchronized to the same time source (hydrogen atomic clock), as depicted in Figure 1, the VLBI and GNSS based time differences should be equal and correspond to the time between the two candidate locations, A and B. In reality, this is not the case, as shown in Figure 2.

The main objective is to analyze the impact of GNSS receiver hardware delays on carrier-phase time transfer with picosecond/millimeter precision and establish local time coherence between GNSS and VLBI [1].

Our proposal (see Figure 3) involves utilizing a ground-based GNSS pseudolite system (ps) synchronized to an optical timing system (H-maser, Hm) developed at the Geodetic Observatory Wettzell, Germany, to calibrate the variable hardware delays of the GNSS receiver. The pseudolite signal has to be synchronized to the optical pulse train (a broadband microwave comb (blue) with equidistant time markers) of the H-maser. We suggest a feedback approach wherein the downconverted pseudolite signal (yellow) and the comb-like phase signal (blue) are compared to determine the required phase delay correction for the GNSS pseudolite local oscillator to align the transmit signal with the H-maser timing signal and calibrate its clock ( $t_{ps}$ ). Any residual hardware delays ( $\delta r_g$ ) could then be estimated via a reformulated iono-free carrier-phase Precise Point Positioning (PPP) approach. Following correction, a 1ps precise clock differencing between VLBI telescopes could be achieved using a classic carrier-phase PPP solution.

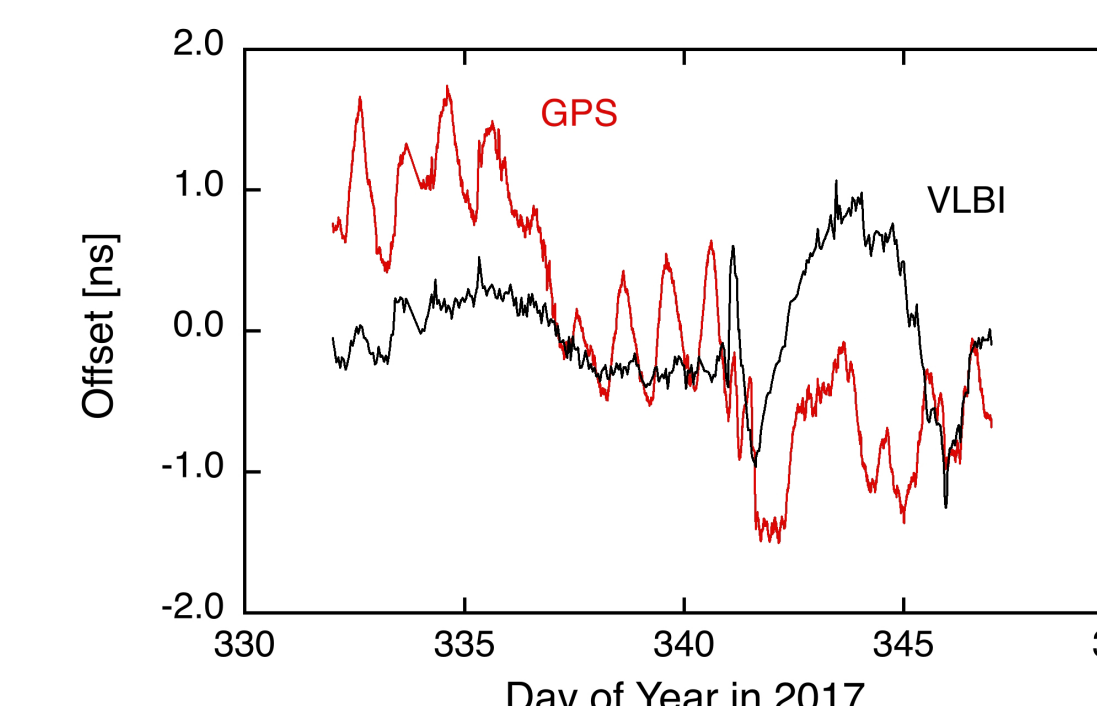


Figure 2: Comparison between the VLBI (black) and GNSS (red) time differences between Wettzell and Matera (990km baseline) over 15 days during 2017. A peak-to-peak variability on the order of 1 ns/30 cm is associated with hardware delays (phase and frequency offsets).

## PROPOSAL

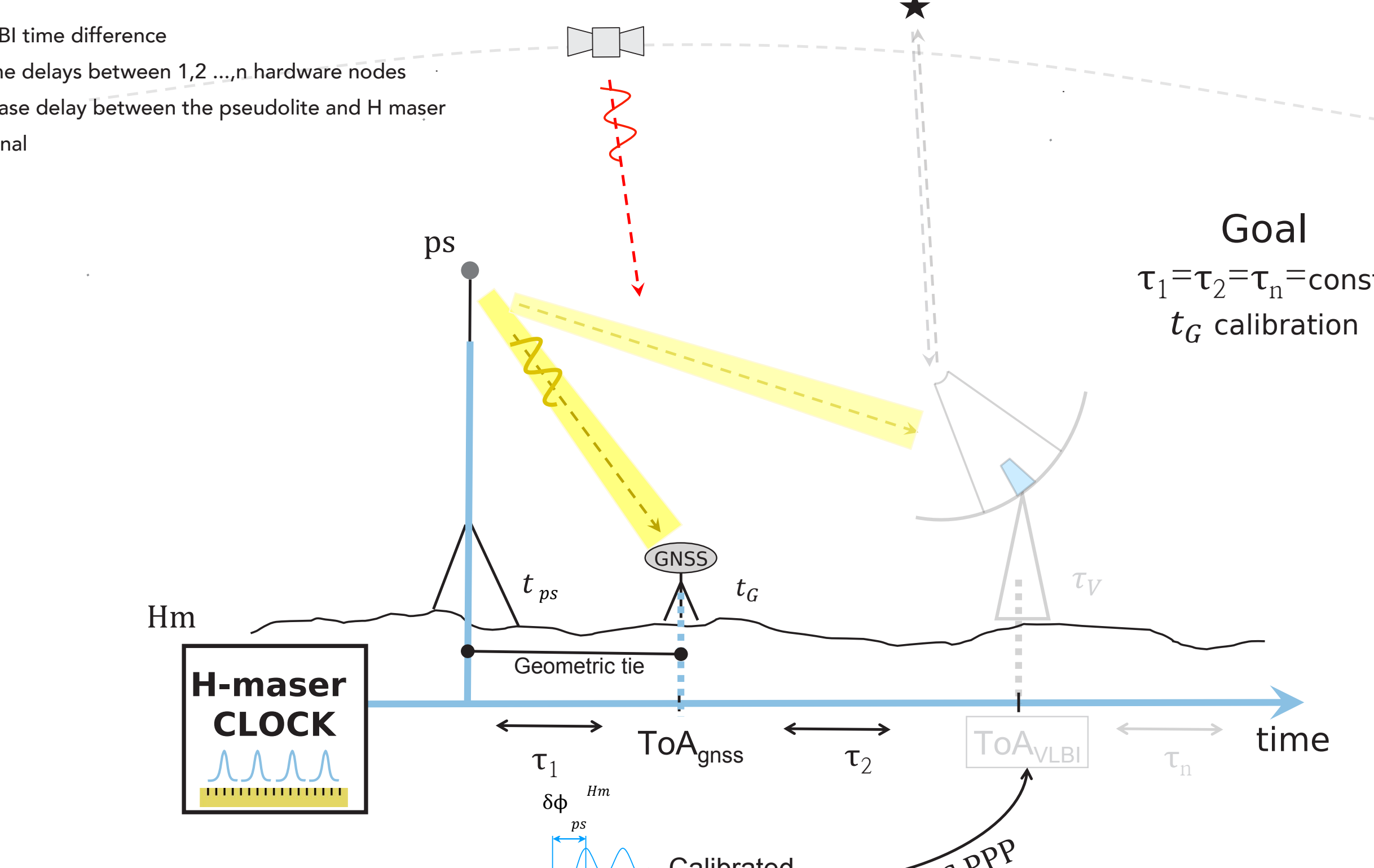


Figure 3: Mitigating variable hardware delays by establishing a calibration of the GNSS and VLBI from the same time source. A GNSS pseudolite (ps) signal (yellow) has to be synchronized with the H-maser broadband microwave comb (blue) with equidistant time markers via a feedback loop approach. The phase delay between the pseudolite and the comb-like signal is used to determine the phase delay correction ( $\delta\phi_{ps}^{Hm}$ ) to calibrate the pseudolite clock and in the end the GNSS receiver clock ( $t_g$ ). Residual hardware delays could then be estimated via PPP (see Section Requirements).

## REQUIREMENTS

Table 1: Hardware requirement inventory for developing a GNSS pseudolite and its trans-receiving chain.

Transmitter	USRP Software Defined Radio with GNURadio implementation	Integer 16 bit IQ sample transmission - PLL int-n mode - Calibration of hardware delays
Receiver	Geodetic grade receiver & (MuSNAT) software defined radio	- Receiver clock errors ( $\delta t_{c_j}^\phi$ ) eliminated via time synchronized pseudolite signal
Transmit antenna	Crossed log-periodic antenna, or helix antenna	- Extremely high directivity (6 dBi gain) - RHCP - Frequency range 1-18 GHz - Hemispherical gain pattern - Calibration of PCO + PCV
Receive antenna	Geodetic antenna with multipath suppression	- High directivity (4.5 dBi gain) - RHCP - Calibrated for PCO + PCV

$$\delta t_{rj}^\phi(t) = \rho_r^\phi(t) + \xi_{rj}^\phi(t) + c(\delta r_{rj} - \delta t_{rj}^\phi) + c(\delta t_{rj}^\phi(t) - \delta t_{rj}^\phi) + \text{relativistic corrections} + \text{atmospheric delays} + \text{wind-up} + \text{residual errors}$$

$$\delta t_{rj}^\phi(t) = \rho_r^\phi(t) + \xi_{rj}^\phi(t) + c(\delta r_{rj} - \delta t_{rj}^\phi) + T_r^s + \lambda N_{rj}^{\text{PS}} + \epsilon_{rj}^{\text{PS}} \quad (2)$$

$$\begin{aligned} \text{Iono-free pseudolite-receiver carrier phase} \\ \phi_{rj}^{\text{PS}}(t) = (\alpha_A \Phi_{rj}^{\text{PS}} + \alpha_B \Phi_{rj}^{\text{PS}}) = P_{rj,\text{IF}}^{\text{PS}}(t) + [\alpha_A \epsilon_{rj}^{\text{PS}}(t) + \alpha_B \epsilon_{rj}^{\text{PS}}(t)] + c[\alpha_A(\delta r_{rA} - \delta r_A^\phi) + \alpha_B(\delta r_{rB} - \delta r_B^\phi)] + \\ = +[\alpha_A \lambda_A N_{rA}^{\text{PS}} + \alpha_B \lambda_B N_{rB}^{\text{PS}}] + [\alpha_A \epsilon_{rA}^{\text{PS}}(t) + \alpha_B \epsilon_{rB}^{\text{PS}}(t)] \end{aligned} \quad (3)$$

$$\begin{aligned} j = A, B \text{ frequencies with } f_A \text{ and } f_B \\ \alpha_A = \frac{f_A^2}{f_B^2} = \frac{f_A^2}{f_A^2 - f_B^2} = \frac{f_A^2}{f_A^2 - f_B^2} \\ \alpha_B = 1 - \frac{f_B^2}{f_A^2 - f_B^2} = \frac{f_A^2}{f_A^2 - f_B^2} \\ P_{rj,\text{IF}}^{\text{PS}}(t) = P_{rj,\text{IF}}^{\text{PS}}(t) + T_{rj}^{\text{PS}}(t) \end{aligned}$$

## EXPERIMENT & RESULTS

Utilizing a USRP-based transmission procedure over free-air, an E1B Galileo signal replica was successfully tracked with an in-house developed GNSS software-defined receiver (SDR). The free-air transmission was planned over the 114 meter distance using a link budget calculation [3] (see Figure 4) such that it will not exceed the allowed

free-air transmission constraints of maximum 30 dB.Hz at critical public areas. Extending the distance from 114 meters to 500 meters, corresponding to the distance from the receiver to a highway, results in a loss of -12.8 dB. To maintain a C/N0 below 30 dB/Hz near critical public areas, a transmission attenuator of 40 dB is recommended.

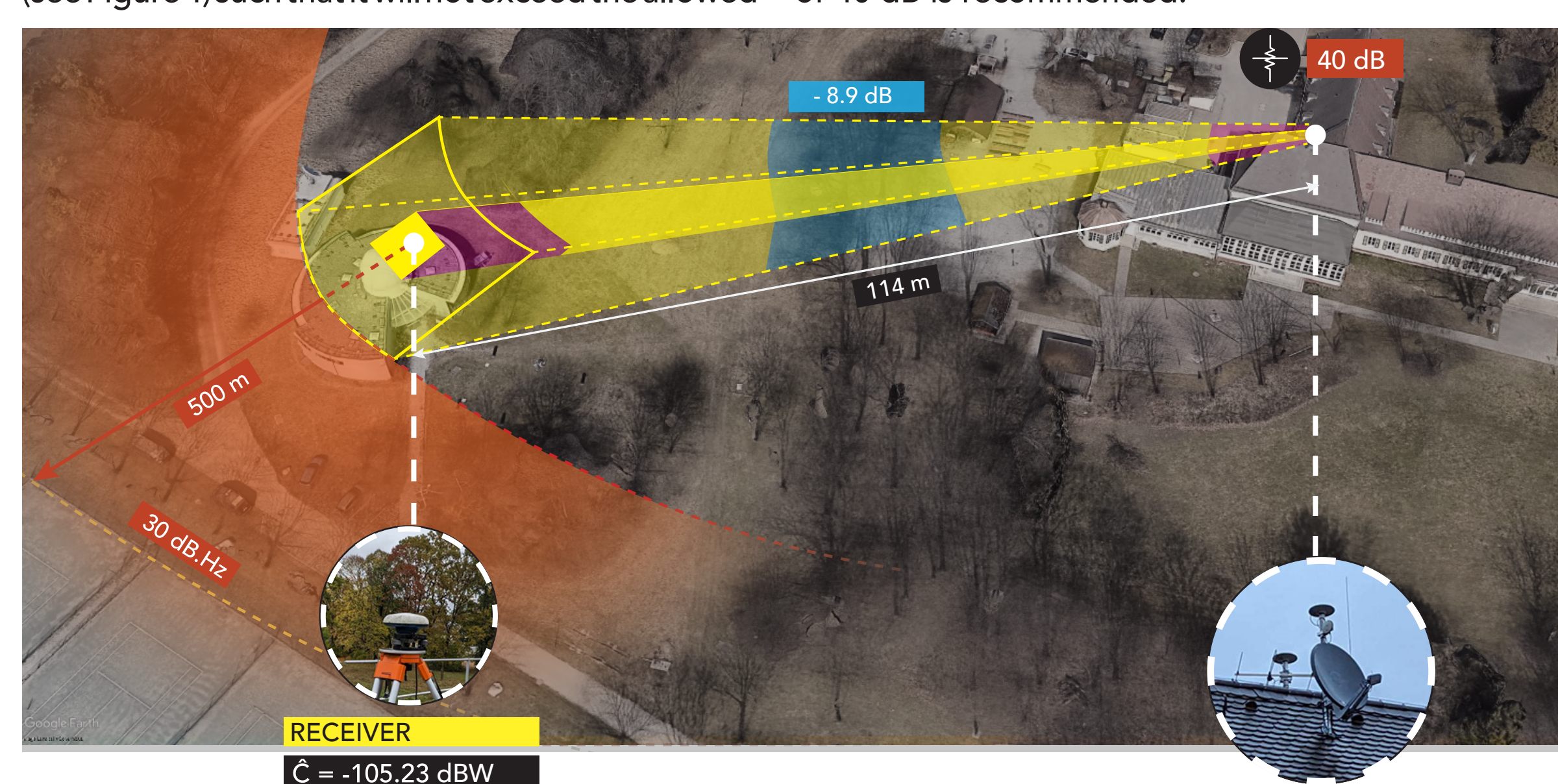


Figure 4: Link budget calculation over the  $r=114$  meters trans-receiver test bed. The estimated direct line-of-sight  $\check{C}/N_0$  of 99.33 dB.Hz is validated against the measured  $C/N_0$  of 87.57 dB.Hz, considering an estimated signal attenuation of -8.9 dB due to the canopy. The residual value of 2.86 dB is attributed to the empirically chosen transmitter ( $G_{T,dB_{ic}}$ ) and receiver antenna gains ( $G_{R,dB_{ic}}$ ) as well as partially measured (%) transmitter cable losses ( $L_{Rr,dB}$ ), and empirically chosen atmospheric and rain loss ( $L_{A,dB}$ ) terms.

## TAKE HOME

1. Hardware delays impact global time transfer; better geometric ties and local time coherence between VLBI and GNSS will improve geodetic reference frames.

2. Use of GNSS pseudolites exploiting the loopback PLL concept can facilitate local time coherence, minimizing variable hardware delays.

3. Attention to hardware, pseudolite signal, and mathematical models is important for minimizing error sources and mitigating variable hardware biases.

4. Ensuring carrier phase stability of trans-receiver testbed is important. Tuning the PLL correctly offers a solution.

Through experimentation with the USRP-based transmitter setup, we identified display oscillations in magnitude and that tuning the Phase-Locked Loop exhibit frequency offset + greater phase noise compared to the int-n mode IQ samples. The increased phase noise likely maintains the carrier frequency stable. A series of static recording campaigns were conducted where a sine wave signal with a central frequency of 1.57001 GHz, sampled at 200 kHz, was fed into the USRP (operating in receiving mode). Both modes were tested in a high-precision carrier-phase-based positioning campaign [4]. The int-n mode resulted in measurements were taken (see Figure 5). In the frac-n mode, the IQ samples

In the frac-n mode, the IQ samples based transmitter setup, we identified display oscillations in magnitude and that tuning the Phase-Locked Loop exhibit frequency offset + greater phase noise compared to the int-n mode IQ samples. The increased phase noise likely maintains the carrier frequency stable. A series of static recording campaigns were conducted where a sine wave signal with a central frequency of 1.57001 GHz, sampled at 200 kHz, was fed into the USRP (operating in receiving mode). Both modes were tested in a high-precision carrier-phase-based positioning campaign [4]. The int-n mode resulted in measurements were taken (see Figure 5). In the frac-n mode, the IQ samples

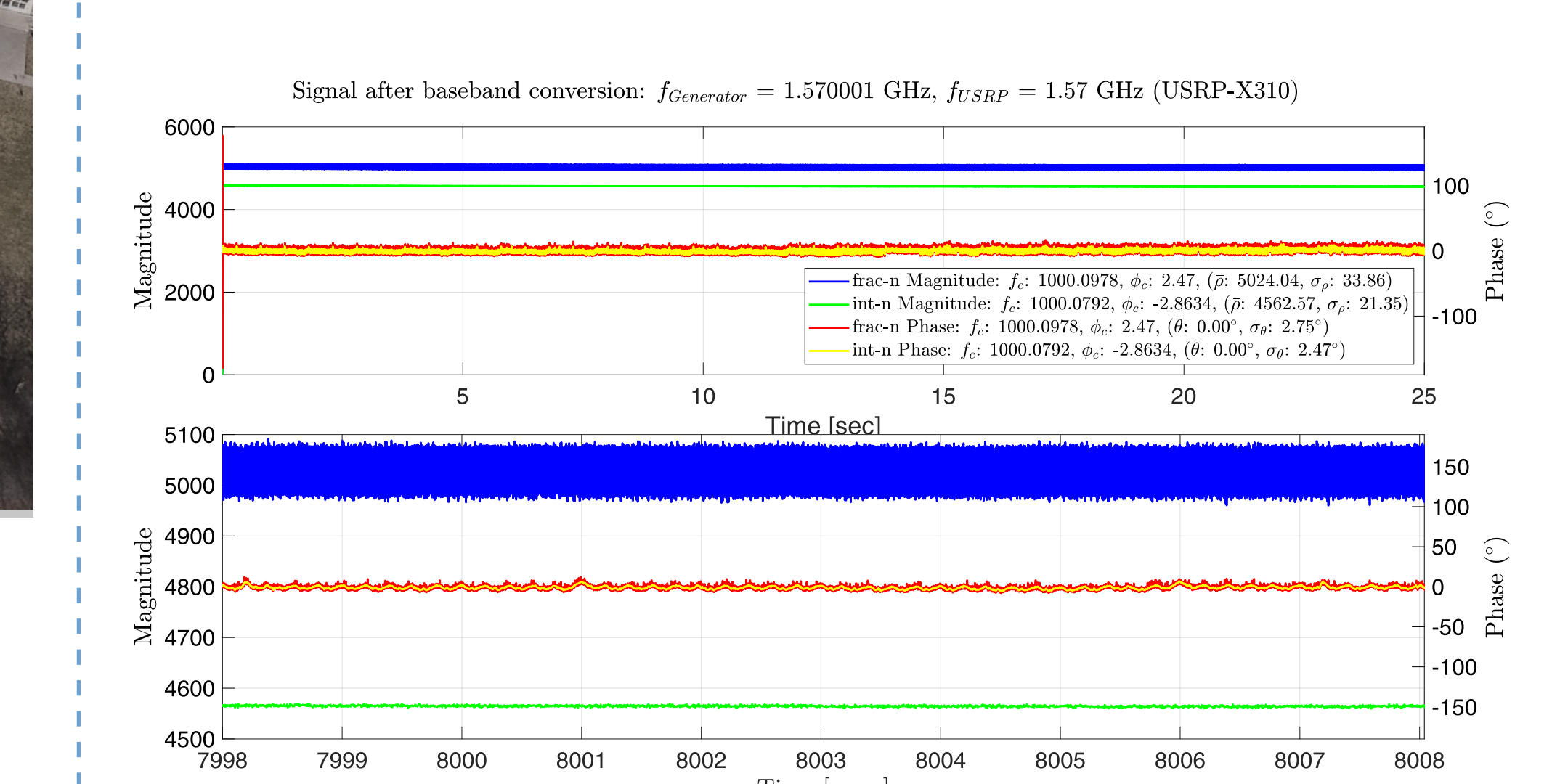


Figure 5: A comparison of the magnitude, frequency and phase characteristics of the IQ samples in int-n (green and yellow) and frac-n (blue and red) mode. The top panel represents a zoomed-in version of the top panel. Tuning the PLL in int-n mode keeps the magnitude + carrier frequency stable.

